Decoupling of stalagmite-derived Asian summer monsoon records from North Atlantic temperature change during marine oxygen isotope stage 5d

Houyun Zhou [a,*], Jianxin Zhao [b], Pingzhong Zhang [c], Chuan-Chou Shen [d], Baoquan Chi [a,e], Yuexing Feng [b], Yin Lin [d], Huazheng Guan [a,e], Chen-Feng You [f]

[a] Guangzhou Institute of Geochemistry, Chinese Academy of Sciences, Guangzhou 510640, China
[b] Radiogenic Isotope Laboratory, Centre for Microscopy and Microanalysis, the University of Queensland, Brisbane, Qld 4072, Australia
[c] Key Laboratory of Western China's Environmental Systems of Ministry of Education, College of Earth and Environment Sciences, Lanzhou University, Lanzhou 730000, China
[d] Department of Geosciences, National Taiwan University, Taipei 106, Taiwan, Republic of China
[e] The Graduate School, Chinese Academy of Sciences, Beijing 100039, China
[f] The Earth Dynamic System Research Center, National Cheng-Kung University, Tainan 701, Taiwan, Republic of China

Abstract

The Asian monsoon is an important component of the global climate system. Seasonal variations in wind, rainfall, and temperature associated with the Asian monsoon systems affect a vast expanse of tropical and subtropical Asia. Speleothem-derived summer monsoon variation in East Asia was previously found to be closely associated with millennial-scale change in temperature in the North Atlantic region between 75 and 10 ka. New evidence recovered from East Asia, however, suggests that the teleconnection between summer monsoon in East Asia and temperature change in the North Atlantic region may have significantly reduced during 120 to ~110 ka, a period directly after the full last interglaciation and corresponding roughly to marine oxygen isotope stage 5d. This reduction may be due to the low ice volume in the North Hemisphere at that time, which makes the millennial-scale change in temperature in the North Atlantic region less effective in influencing the Asian summer monsoon. This is important for investigating the mechanisms controlling the Asian summer monsoon and the paleoclimatic teleconnection between East Asia and the North Atlantic region, and for predicting monsoon-associated precipitation in East Asia under a global-warming trend.
© 2008 University of Washington. All rights reserved.

Keywords: Asian monsoon; North Atlantic; Stalagmite; Paleoclimate; Millennial-scale event; Decoupling; Teleconnection; Marine oxygen isotope stage 5d

Introduction

The Asian Monsoon is an important component of the global climate system. Precipitation associated with the Asian summer monsoon (ASM) supports the agriculture and more than half of the world population in East Asia. Understanding the mechanism(s) controlling the ASM is important not only for paleoclimatic investigation but also for social and economic development in this region. Investigation on speleothems from Hulu Cave (32°30′N, 119°10′E) (Wang et al., 2001) and Dongge Cave (25°17′N, 108°5′E) (Yuan et al., 2004) (see Fig. 1 for locations of the two caves) revealed that variation of the ASM was closely related to millennial-scale change in temperature in the North Atlantic region during the period from 75 to 10 ka (Dansgaard et al., 1993; Grootes et al., 1993; NGRIP Project members, 2004). Lower temperature in the North Atlantic region, which is recorded by lighter stable oxygen isotopic composition ($\delta^{18}O$) in Greenland ice core, is associated with weaker summer monsoon in East Asia recorded by speleothem with higher $\delta^{18}O$ and vice versa. Speleothem-derived ASM records for the Holocene also reveal that some weak ASM events are in correspondence with ice-rafting and cold events, e.g. the 8.2-ka cold event, in the North Atlantic region (Wang et al., 2005). Before 75 ka, however,

* Corresponding author. Guangzhou Institute of Geochemistry, Chinese Academy of Sciences. No. 511, Kehua Street, Guangzhou, Guangdong Province, 510640, China. Fax: +86 20 8529 0130.
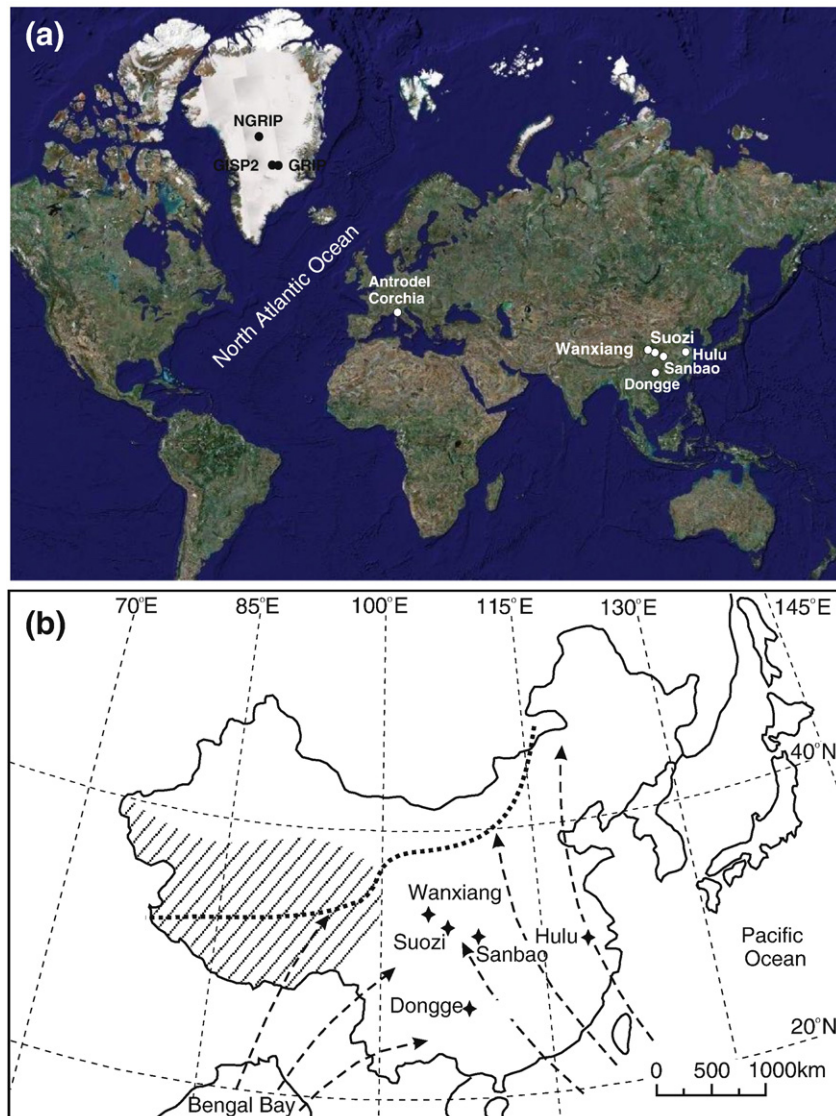*E-mail address:* hyzhou@gig.ac.cn (H. Zhou).

Figure 1. (a) Distribution of the GRIP (72.5°N, 37.3°W), GISP2 (72.5°N, 38.3°W) and NGRIP (75.10°N, 42.32°W) ice cores (Dansgaard et al., 1993; Grootes et al., 1993; NGRIP Project members, 2004), Antro del Corchia Cave (44°2′N, 10°17′E) (Drysdale et al., 2007) and the five karstic caves in East Asia discussed in the text, including Hulu Cave (32°30′N, 119°10′E) (Wang et al., 2001), Dongge Cave (25°17′N, 108°05′E) (Yuan et al., 2004; Kelly et al., 2006), Wanxiang Cave (33°19′N, 105°00′E) (Johnson et al., 2006), Sanbao Cave (31°40′N, 110°26′E) (Wang et al., 2008) and Suozi Cave (32°26′N, 107°10′E) (this study). (b) An enlargement of East Asia. In (b), the dashed arrows indicate sources and tracks of moisture transportation during the summer season; the thick dashed line indicates the northwestern limit of the East Asian summer monsoon; and the hatched area is the Qinghai–Tibet Plateau.

it is not as clear whether the millennial-scale temperature changes in the North Atlantic region exert significant influence on the ASM (Johnson et al., 2006; Kelly et al., 2006), as was found between 75 and 10 ka (Wang et al., 2001; Yuan et al., 2004). For example, Kelly et al. (2006) found that while the Greenland interstadial periods (GIS) 23 and 24 were archived in the D3 $\delta^{18}O$ record from Dongge Cave, the GIS 25 did not show evident imprint in this record. This observation suggests that the teleconnection between the ASM and temperature change in the North Atlantic region may have changed temporally. However, it is not clear whether the absence of GIS 25 in the Dongge $\delta^{18}O$ record is a site specific or a regional phenomenon. In addition, the chronology of Greenland ice core needs validation with precisely dated radiogenic chronology. With new speleothem $\delta^{18}O$ records recovered, the absence or very weak-

ness of GIS 25 event is illustrated in the speleothem-derived ASM records from a wide geographical distribution in China (Johnson et al., 2006; Kelly et al., 2006; Wang et al., 2008; this study). This suggests that during marine oxygen isotope stage (MIS) 5d at 120–110 ka, a short period directly after the full last interglaciation, MIS 5e, at 130–120 ka (Yuan et al., 2004; Kelly et al., 2006), the millennial-scale temperature change in the North Atlantic region may have exerted much less influence on the ASM variations relative to the period from 75 to 10 ka.

North Atlantic temperature change, 120 to 100 ka

The temperature change in the North Atlantic region is well represented with ice core $\delta^{18}O$ records in Greenland. Several ice cores have been recovered in Greenland, among which include

the two frequently referenced cores drilled at the beginning of the 1990s in central Greenland, i.e. GRIP (Dansgaard et al., 1993) and GISP2 (Grootes et al., 1993), and the recently recovered NGRIP ice core (NGRIP Project members, 2004) which is from ~325 km north of GRIP and GISP2 (Fig. 1). The chronologies for the period of MIS 5d in the two former cores are not well evaluated due to the disturbance near the bottom 10% of the cores owing to ice folding close to the bedrock (Grootes et al., 1993; Chappellaz et al., 1997; Johnsen et al., 1997). The age model for NGRIP is comparatively reliable and further constrained with a high-resolution dated speleothem $\delta^{18}O$ record in a stalagmite, CC28, collected from Antro del Corchia Cave (44°2′N, 10°17′E; Fig. 1) in Italy (Drysdale et al., 2007).

The CC28 $\delta^{18}O$ record documents past climate and environment changes with its high value corresponding to cold and dry climate and vice versa. Similar to the Greenland ice cores,

the CC28 $\delta^{18}O$ record provides a high-resolution record of temperature change in the North Atlantic region (Drysdale et al., 2007). Consistency between CC28 and NGRIP $\delta^{18}O$ records within dating errors gives a strong support to the NGRIP chronology at MIS 5d-c (Fig. 2) (NGRIP Project members, 2004; Drysdale et al., 2007). During 120 to 100 ka, the temperature variations in the North Atlantic region display significant millennial-scale fluctuations, characterized with three warm interstades (GIS23 to 25) and three cold stades (GS24 to 26) in the NGRIP ice core (NGRIP Project members, 2004) (Fig. 2). In the CC28 $\delta^{18}O$ record, three cold events, including C23 and C24 identified by Drysdale et al. (2007) and C25 identified here, correspond to these stades in the NGRIP ice core (Fig. 2). These cold events were also recorded in other continental and marine sediments in the North Atlantic region (Drysdale et al., 2007 and reference therein).
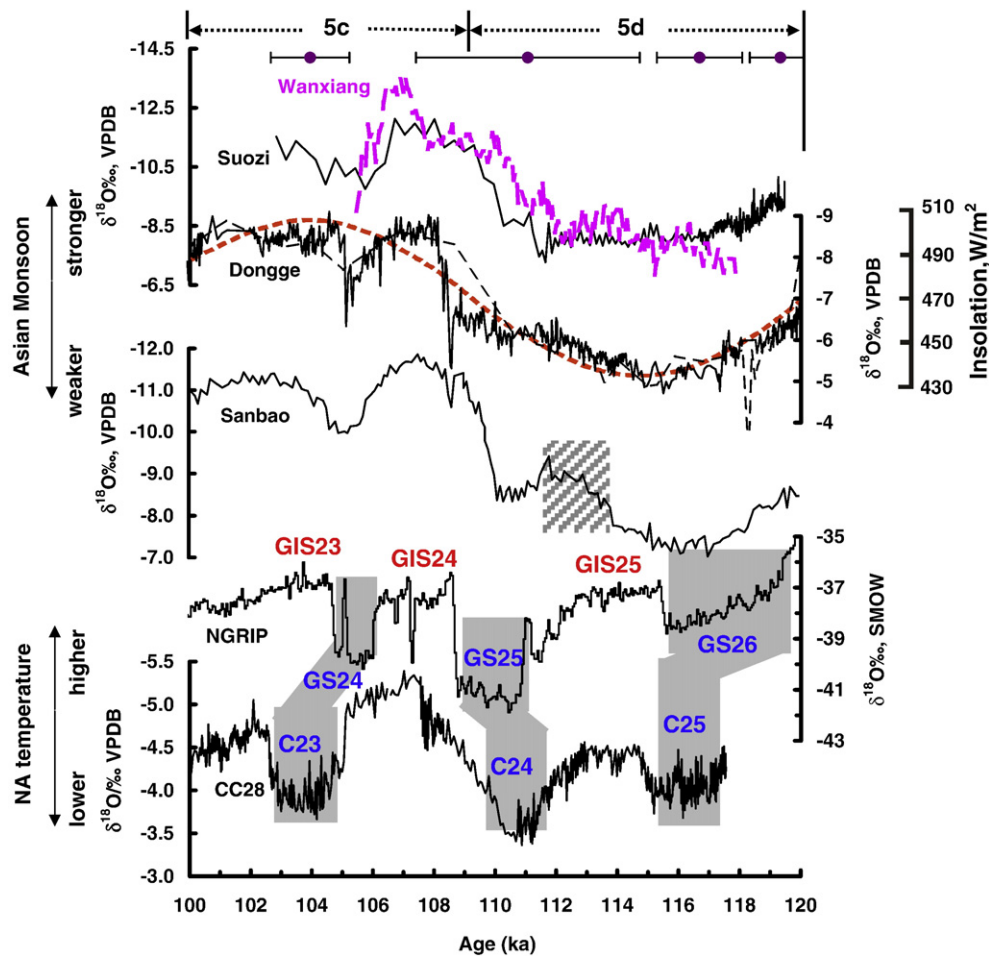

Figure 2. Comparison of the speleothem-derived ASM variations with temperature changes in the North Atlantic region during MIS 5d-c. The ASM variations are archived in the speleothem $\delta^{18}O$ records from Suozi Cave, Central China (this study), Wanxiang Cave, Central China (Johnson et al., 2006), Sanbao Cave, Central China (Wang et al., 2008) and Dongge Cave, Southwest China (Yuan et al., 2004; Kelly et al., 2006). In the Dongge records, the thin dashed line represents the low-resolution version published in 2004 (Yuan et al., 2004); the thin solid line represents the high-resolution version revised later (Kelly et al., 2006). The temperature changes in the North Atlantic region are represented by the $\delta^{18}O$ records of the NGRIP ice core from Greenland (NGRIP Project members, 2004) and CC28 stalagmite from Antro del Corchia Cave in Italy (Drysdale et al., 2007). Also shown for comparison is the curve of the integrated summer insolation at 25°N over the months of June, July and August (Berger, 1978) (thick dashed line plotted together with the Dongge records). GIS23 to 25 represent Greenland interstadials 23 to 25, while GS24 to 26 denote Greenland stadials 24 to 26 (NGRIP Project members, 2004). C23 to 25 represent three cold events archived in North Atlantic marine and continental records (Drysdale et al., 2007 and reference therein). The hatched rectangle on the Sanbao record indicates a weak ASM peak (Wang et al., 2008) probably associated with GIS 25. The horizontal bars on the top of the Suozi and Wanxiang plot indicate U-Th dates and 2-sigma uncertainties for the Suozi $\delta^{18}O$ record. The Suozi and Wanxiang $\delta^{18}O$ records are plotted on the same scale because they are relatively closer to the northwest boundary of the ASM and display roughly similar $\delta^{18}O$ ranges.
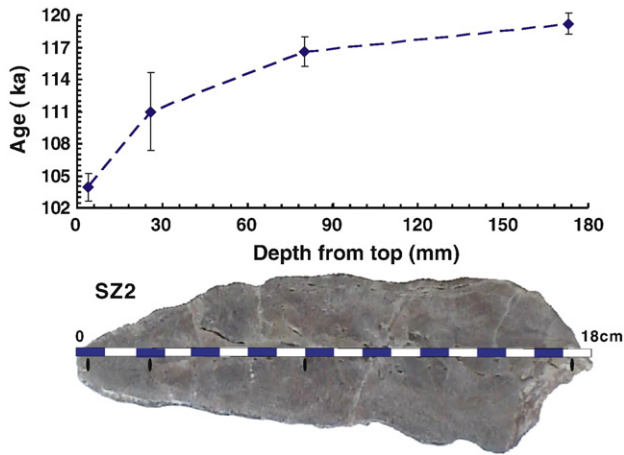
Figure 3. Stalagmite SZ2 and its age model. The scale bar is shown on the image of SZ2. It also represents the route along which the sub-samples for oxygen and carbon isotopic analysis were collected. The four small black ellipses below the scale indicate the locations where sub-samples for TIMS U-Th dating were obtained.

Speleothem-derived Asian summer monsoon records during MIS 5d-c

Except for the D3 $\delta^{18}O$ record from Dongge Cave (Yuan et al., 2004; Kelly et al., 2006), there are some other speleothem-derived ASM records covering MIS 5d, including the WXSM52 record from Wanxiang Cave (33°19′N, 105°00′E) (Johnson et al., 2006), the recently published SB23 record from Sanbao Cave (31°40′N, 110°26′E) (Wang et al., 2008), and a newly obtained speleothem $\delta^{18}O$ record reconstructed from a stalagmite collected from Suozi Cave (32°26′N, 107°10′E) in Central China (see Fig. 1 for the locations of these caves) (Fig. 2). Suozi Cave is located in northeast Sichuan province, Central China (Fig. 1). This site experiences a typical Asian monsoon climate at present with an annual mean temperature of ~15 °C and an annual mean precipitation of ~1100 mm. Most of the precipitation falls in summer season (Sinomaps Press, 1984). Suozi Cave has a very small entrance to allow only one person to climb into or out of the cave at one time. Stalagmite SZ2 was collected from a site more than 100 m deep from the entrance. The host rock of Suozi Cave comprises Late Permian limestone (Bureau of Geology and Mineral Resources of Sichuan Province, 1991). The overlying soil layer above the cave is

usually thin, less than 30 cm thick, or even absent in places. Local vegetation consists mainly of trees including pine, cypress and some deciduous broadleaf species.

SZ2 is ~18 cm in length. Like most other stalagmites, it is thicker at the base than at the top (Fig. 3). The stalagmite was halved along its growth axis and the exposed cut surface shows that the stalagmite looks a little more brownish below a depth of ~28 mm from the top. Visual and microscopic examinations suggest that the carbonate in SZ2 should be composed of calcite. Four horizons, shown in Figure 3, were drilled for TIMS U-Th dating using the method described by Zhao et al. (2001) in the Radiogenic Isotope Laboratory, the University of Queensland (Table 1). These ages show that SZ2 developed from 120 to 103 ka, a period directly after the full last interglacial (Yuan et al., 2004; Kelly et al., 2006), and suggest that its growth rate decreased upwards (Fig. 3). No growth hiatus is apparent on the cut surface. A first-order chronology was therefore established by linear interpolation between dated points (Fig. 3). Sub-samples for $\delta^{18}O$ and $\delta^{13}C$ analysis were collected in the same way as described in Zhou et al. (2008). The sub-sampling interval is ~100 μm. One out of ten collected sub-samples from every millimeter, at the start of each millimeter, was chosen for C–O isotope analysis, and a total of 178 sub-samples were analyzed. The C–O isotope analysis was conducted on a GV IsoPrime II stable IRMS coupled with online carbonate preparation system at the Key Laboratory of Geochemistry and Geochronology of Guangzhou Institute of Geochemistry. About 50 μg of powdered carbonate was used. The C–O isotope data are reported conventionally as $\delta^{18}O$ and $\delta^{13}C$ in ‰ relative to the Vienna Peedee Belemnite (VPDB) standard. Analytical errors are <0.12‰ (2σ) for $\delta^{18}O$ and <0.06‰ (2σ) for $\delta^{13}C$, respectively.

The SZ2 $\delta^{18}O$ record, ranging from −12.1‰ to −8.0‰, is characterized with a depleted ^{18}O shift of ~3‰ from 110 to 109 ka (Fig. 2). Before this shift, $\delta^{18}O$ values gradually increased from −9.6‰ to −8.0‰ during 120–110 ka. After the shift, the $\delta^{18}O$ record displays a notable increase between 106 to 105 ka, which makes the $\delta^{18}O$ variation during 110–103 ka similar to the double peak seen in the Dongge and Sanbao records (Yuan et al., 2004; Kelly et al., 2006; Wang et al., 2008) (Fig. 2).

Although the Hendy Test (Hendy, 1971) was not carried out on SZ2, the following evidence suggest that carbonates in SZ2 should be precipitated in isotopic equilibrium: (1) SZ2 was

Table 1
TIMS U-series isotopic results and ages for stalagmite SZ2 from Suozi Cave, Central China

Sample name	Distance from top (mm)	U (ppm)	±2σ	^{232}Th (ppb)	±2σ	$^{230}Th/^{232}Th$	$^{230}Th/^{238}U$	±2σ	$^{234}U/^{238}U$	±2σ	Uncorrected ^{230}Th age (ka)	±2σ	Corrected ^{230}Th age (ka)	±2σ	Corrected initial $^{234}U/^{238}U$	±2σ
SZ2-004	4	0.2252	0.0001	13.2	0.1	61.4	1.181	0.008	1.801	0.002	104.7	1.1	103.9	1.3	2.092	0.008
SZ2-026	26	0.2443	0.0002	64.3	0.5	13.7	1.189	0.008	1.716	0.002	115.0	1.3	111.0	3.6	2.056	0.032
SZ2-080	80	0.3306	0.0003	23.2	0.2	50.4	1.167	0.006	1.665	0.002	117.7	1.1	116.6	1.4	1.943	0.008
SZ2-173	173	0.2424	0.0002	11.1	0.1	76.4	1.155	0.004	1.631	0.003	119.9	0.8	119.2	1.0	1.896	0.006

Ratios listed in the table refer to activity ratios normalized to the corresponding ratios measured for the secular-equilibrium HU-1 standard, which is independent of decay constants used. ^{230}Th ages are calculated using Isoplot Excel Version. Non-radiogenic ^{230}Th correction was made assuming non-radiogenic component Th/U=3.8±1.9 (average crustal value, equivalent to a $^{230}Th/^{232}Th$ ratio of ≈0.83±0.41), and ^{238}U, ^{234}U, ^{232}Th and ^{230}Th are in secular equilibrium. This non-radiogenic correction results in large age error magnification for samples with low $^{230}Th/^{232}Th$ ratios, e.g. for SZ2-026.

sampled from Suozi Cave in depth, which has only a very small entrance; (2) the trend of the SZ2 $\delta^{18}O$ record is similar to those obtained in the ASM regime (Fig. 2); and (3) the $\delta^{18}O$ and $\delta^{13}C$ of SZ2 do not show a positive correlation, as would be expected if kinetic fractionation occurred (Hendy, 1971). Instead, a negative correlation between $\delta^{18}O$ and $\delta^{13}C$ can be observed (Fig. 4). On the other hand, the large shift in $\delta^{18}O$ cannot be attributed to cave temperature change. For instance, if the $\delta^{18}O$ of SZ2 was controlled by temperature-related calcite–water isotopic fractionation, a ~3‰ shift of $\delta^{18}O$ would suggest a temperature change of ~13 °C during the MIS 5d-c transition, which seems unlikely and in sharp contrast to the sedimentary proxy records in the East China Sea and Pacific with an inferred sea surface temperature change of ~1 °C during the MIS 5d-c transition (Lea et al., 2000; Zhou et al., 2007). The parallelism of the Suozi $\delta^{18}O$ record to those obtained in the ASM regime (Fig. 2) suggests that the Suozi $\delta^{18}O$ record is a good replication

of the other records and therefore can be used as an appropriate proxy for the ASM variations. Thus in the following discussion, we interpret the $\delta^{18}O$ of SZ2 in terms of the ASM variations as commonly assumed in many speleothem-based ASM investigations (Wang et al., 2001, 2005, 2008; Yuan et al., 2004; Dykoski et al., 2005; Johnson et al., 2006; Kelly et al., 2006; Hu et al., 2008).

The Suozi $\delta^{18}O$ record is systematically lower than the Dongge records (Yuan et al., 2004; Kelly et al., 2006) (Fig. 2). A similar difference is also observed between the Dongge and Wanxiang records (Johnson et al., 2006) (Fig. 2). These are in accordance with pervious investigations which revealed that on the Chinese land mass, the $\delta^{18}O$ values for contemporaneous stalagmites usually decrease from south to north and/or from east to west (Wang et al., 2001, 2008; Yuan et al., 2004; Tan and Cai, 2005; Hu et al., 2005; Johnson et al., 2006; Shao et al., 2006). This is also consistent with the $\delta^{18}O$ distribution of modern precipitation (Zhang and Yao, 1998), which is related with vapor source (Johnson et al., 2006) and continental effect (or "rainout effect") (Dansgaard, 1964).

More interesting is the coherence between the Suozi $\delta^{18}O$ record and other speleothem-derived ASM records. For example, the similarity among the Suozi, Wanxiang (Johnson et al., 2006) and the low-resolution Dongge record (Yuan et al., 2004) is excellent (Fig. 2). As to the revised high-resolution Dongge record (Kelly et al., 2006), its general trend is also parallel to the Suozi and Wanxiang records although it shows a $\delta^{18}O$ shift ~1 ka later during MIS 5d-c transition relative to the low-resolution Dongge record (Yuan et al., 2004) (Fig. 2). All the four speleothem-derived ASM curves, including the low- and high-resolution Dongge $\delta^{18}O$ records (Yuan et al., 2004; Kelly et al., 2006), the Wanxiang (Johnson et al., 2006) and Suozi (this study) $\delta^{18}O$ records, show variations with relatively small amplitude and do not document any evident peak ASM event during MIS 5d (Fig. 2). This is somewhat different from the newly published Sanbao $\delta^{18}O$ record (Wang et al., 2008) which displays a small $\delta^{18}O$ negative excursion, suggesting a weak ASM-strengthening event centered at ~113 ka (Fig. 2). However, the overall trend of the Sanbao record is coherent with other speleothem $\delta^{18}O$ records during MIS 5d-c (Fig. 2). While we recognize that age uncertainties of the speleothem $\delta^{18}O$ records (Johnson et al., 2006; Kelly et al., 2006; Table 1) preclude an exact temporal correlation, a high similarity exists in their trends (Fig. 2) and suggests the validity of the SZ2 age model established with four ^{230}Th dates (Table 1; Fig. 3).

The speleothem-derived ASM records illustrated in Figure 2 have a wide geographical distribution, e.g. Suozi and Wanxiang caves are much inland and close to the northwest boundary of the ASM relative to the Dongge Cave (Fig. 1-B). Thus the $\delta^{18}O$ records from all the four caves can be used to infer a regional, rather than a site specific, ASM climate. Based on these records, it can be inferred that, during MIS 5d, the ASM was relatively weak and fluctuated only at small amplitude, with a weak ASM-strengthening event being archived only in the Sanbao record. After the transition to MIS 5c, the ASM strengthened significantly and fluctuated at larger amplitude. $\delta^{18}O$ shift corresponding to this transition is greater than 2.5‰ in all the

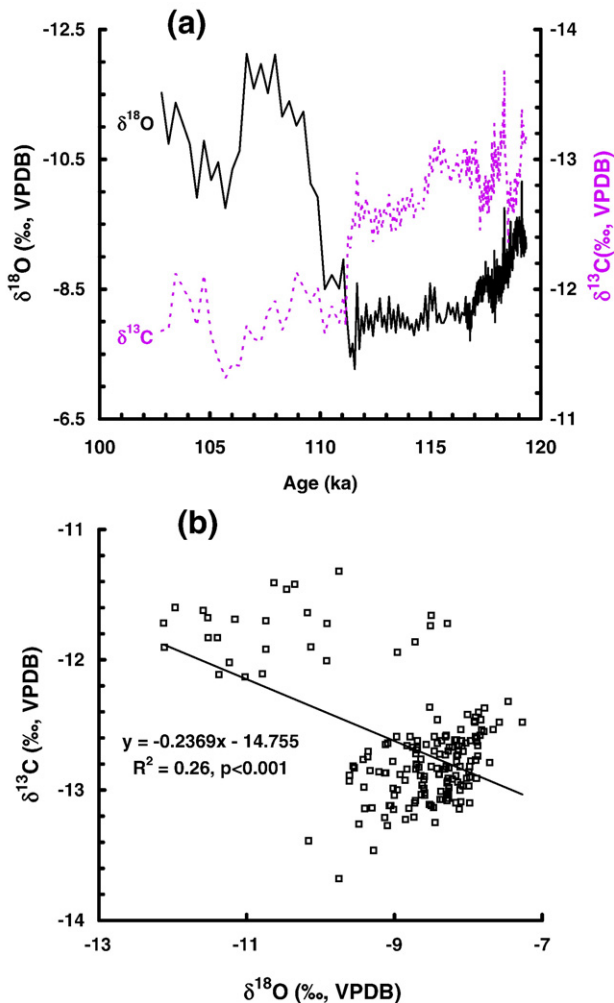Figure 4. The temporal variation of the oxygen and carbon isotopic compositions ($\delta^{18}O$ and $\delta^{13}C$) of SZ2 (a) and their correlation (b). The $\delta^{18}O$ and $\delta^{13}C$ data for SZ2 do not show a positive correlation. Rather, they appear to display a negative correlation with a R^2 value of 0.26. According to the Hendy Test (Hendy, 1971), the carbonates in SZ2 should be precipitated under isotopic equilibrium and the $\delta^{18}O$ and $\delta^{13}C$ data of SZ2 could be used as proxies for past climate and environment.

speleothem δ^{18}O records (Fig. 2). A weak ASM event centered at ~105 ka was evident, making the ASM variations a double peak during MIS 5c (Fig. 2).

Decoupling of the Asian summer monsoon from North Atlantic temperature

The ASM records archived in the four caves (Dongge, Sanbao, Suozi and Wanxiang) are compared systematically with the temperature change in the North Atlantic region documented by the NGRIP and CC28 δ^{18}O records (Fig. 2). The monsoon records appear to show a trend much different from the temperature change. Especially the millennial-scale events during MIS 5d that are apparent in temperature change in the North Atlantic region do not show evident signals, at least are much weak, in the monsoon records. The GIS 25 event, which suggests a temperature as warm as in GIS 24 and 23 in the NGRIP δ^{18}O record, is almost absent in the Dongge, Suozi and Wanxiang δ^{18}O records (Fig. 2). Although the Sanbao record shows a negative δ^{18}O excursion corresponding to this event, the associated δ^{18}O values average ca. −9‰, remarkably higher than those associated with the GIS 24 and 23 events which average ca. −11.5‰ and −11‰, respectively. This suggests a much weaker ASM associated with GIS 25 than with the other two events (Fig. 2). As a whole, the speleothem-derived ASM records during MIS 5d-c show a much closer correlation with the northern hemisphere insolation than with the temperature change in the North Atlantic region (Fig. 2), suggesting that the ASM during this period appears to be dominated by solar insolation rather than by the millennial-scale temperature change in the North Atlantic region.

This scenario is very different from the situation revealed by the Hulu and Dongge records during 75 to 10 ka when the millennial-scale temperature change in the North Atlantic region is at least as equally important as north hemisphere insolation in affecting the ASM (Wang et al., 2001; Yuan et al., 2004). Wang et al. (2001) suggested that speleothem-derived ASM was related mainly to orbitally controlled changes in insolation and circulation changes internal to the climate system. The millennial-scale temperature change in the North Atlantic region may influence both the Asian summer and winter monsoons through rapidly reorganizing oceanic/atmospheric circulation patterns in northern hemisphere (Porter and An, 1995; Wang et al., 2001).

As illustrated in Figure 2, the insolation signal was clearly displayed in the ASM records during MIS 5d-c. We speculate that one possible mechanism for the absence or weak presence of the GIS 25 event in the ASM records (Fig. 2) may be related to this reorganization. As simulated by Wang and Mysak (2006), the warming and cooling associated with D–O oscillations are amplified by changes of sea-ice extent. Low ice volume in the Northern Hemisphere would lead to a less amplification of temperature change. In particular, the temperature change associated with D–O oscillations is much smaller over the continental Eurasia than in the North Atlantic region. Another plausible mechanism may be that a low ice volume favors an atmospheric circulation more zonal and less meridional (Wang et al., 2001) and thus makes the temperature

change in the North Atlantic region less effective in affecting the ASM. The decoupling of the ASM from the millennial-scale temperature change in the North Atlantic region during MIS 5d (Fig. 2) may be related with the low ice volume during a short period after the full last interglacial (Martinson et al., 1987; Shackleton, 1987). During the Holocene, which has a similar ice volume as the last interglacial (Martinson et al., 1987; Shackleton, 1987), although some cold events such as the one at 8.2 ka were propagated from the North Atlantic region to the ASM regime, some ASM-weakening events, especially the remarkable one at ~4 ka (Wu and Liu, 2004), do not show their counterparts in the Greenland temperature records (Wang et al., 2005). In addition, the ASM weakens greatly during late Holocene (Dykoski et al., 2005; Wang et al., 2005), indicating an overall trend parallel with solar insolation rather than with temperature change in the North Atlantic region. This suggests a notably reduced teleconnection between the ASM and North Atlantic temperature during the Holocene relative to the period from 75 to 10 ka (Wang et al., 2001; Yuan et al., 2004). Barnett et al. (1989) pointed out that interannual variability in Eurasian snow cover may also influence the intensity of the ASM. However, it is not clear at present whether the Eurasian snow cover was involved in the decoupling of the ASM and North Atlantic temperature at MIS 5d as shown in Figure 2. In conclusion, this study reveals that not all the millennial-scale temperature change identified in the North Atlantic region exerts significant influence on the ASM. The summer monsoon system may operate relatively independently and respond mainly to solar insolation if the ice volume in the North Hemisphere is low. This study also provides critical information for investigating the mechanisms controlling the ASM and the paleoclimatic teleconnection between East Asia and the North Atlantic region, and for predicting monsoon-associated precipitation in East Asia under a global-warming trend. However, the mechanisms for the decoupling, or at least a much weak teleconnection between the East Asia summer monsoon and temperature change in the North Atlantic region during MIS 5d (Fig. 2) are speculative and warrant further investigation.

References

Barnett, T.P., Dümenil, L., Schlese, U., Roeckner, E., Latif, M., 1989. The effect of Eurasian snow cover on regional and global climate variations. J. Atmos. Sci. 46, 661–685.

Berger, A.L., 1978. Long-term variations of caloric insolation resulting from the Earth's orbital elements. Quat. Res. 9, 139–167.

Bureau of Geology and Mineral Resources of Sichuan Province, 1991. Regional Geology of Sichuan Province. Geological Publishing House, Beijing.

Chappellaz, J., Brook, E., Blunier, T., Malaize, B., 1997. CH_4 and $\delta^{18}O$ of O_2 records from Antarctic and Greenland ice: a clue for stratigraphic disturbance in the bottom part of the Greenland Ice Core Project and Greenland Ice Sheet Project 2 ice cores. J. Geophys. Res. 102, 26547–26557.

Dansgaard, W., 1964. Stable isotopes in precipitation. Tellus 16 (4), 436–468.

Dansgaard, W., Johnsen, S.J., Clausen, H.B., Dahl-Jensen, D., Gundestrup, N.S., Hammer, C.U., Hvidberg, C.S., Steffensen, J.P., Sveinbjörnsdottir, A.E., Jouzel, J., Bond, G., 1993. Evidence for general instability of past climate from a 250-kyr ice-core record. Nature 364, 218–220.

Drysdale, R.N., Zanchetta, G., Hellstrom, J.C., Fallick, A.E., McDonald, J., Cartwright, I., 2007. Stalagmite evidence for the precise timing of North Atlantic cold events during the early last glacial. Geology 35, 77–80.

Dykoski, C.A., Edwards, R.L., Cheng, H., Yuan, D.X., Cai, Y.J., Zhang, M.L., Lin, Y.S., Qin, J.M., An, Z.S., Revenauh, J., 2005. A high-resolution, absolute-dated Holocene and deglacial Asian monsoon record from Dongge Cave, China. Earth Planet. Sci. Lett. 233, 71–86.

Grootes, P.M., Stuiver, M., White, J.W.C., Johnsen, S.J., Jouzel, J., 1993. Comparison of oxygen isotope records from the GISP2 and GRIP Greenland ice cores. Nature 366, 552–554.

Hendy, C.H., 1971. The isotopic geochemistry of speleothems 1: the calculation of the effects of the different modes of formation on the isotopic composition of speleothems and their applicability as palaeoclimatic indicators. Geochim. Cosmochim. Acta 35, 801–824.

Hu, C.Y., Huang, J.H., Fang, N.Q., Xie, S.C., Henderson, G.M., Cai, Y.J., 2005. Adsorbed silica in stalagmite carbonate and its relationship to past rainfall. Geochim. Cosmochim. Acta 69, 2285–2292.

Hu, C.Y., Henderson, G.M., Huang, J.H., Xie, S.C., Sun, Y., Johnson, K.R., 2008. Quantification of Holocene Asian monsoon rainfall from spatially separated cave records. Earth Planet. Sci. Lett. 266, 221–232.

Johnsen, S.J., Clausen, H.B., Dansgaard, W., Gundestrup, N.S., Hammer, C.U., Andersen, U., Andersen, K.K., Hvidberg, C.S., Dahl-Jensen, D., Steffensen, J.P., Shoji, H., Sveinbjörnsdóttir, Á.E., White, J., Jouzel, J., Fishe, D., 1997. The $\delta^{18}O$ record along the Greenland Ice Core Project deep ice core and the problem of possible Eemian climatic instability. J. Geophys. Res. 102, 26397–26410.

Johnson, K.R., Ingram, B.L., Sharp, W.D., Zhang, P.Z., 2006. East Asian summer monsoon variability during Marine Isotope Stage 5 based on speleothem $\delta^{18}O$ records from Wanxiang Cave, Central China. Palaeogeogr. Palaeoclimatol. Palaeoecol. 236, 5–19.

Kelly, M.J., Edwards, R.L., Cheng, H., Yuan, D.X., Cai, Y.J., Zhang, M.L., Lin, Y.S., An, Z.S., 2006. High resolution characterization of the Asian Monsoon between 146,000 and 99,000 years B.P. from Dongge Cave, China and global correlation of events surrounding Termination II. Palaeogeogr. Palaeoclimatol. Palaeoecol. 236, 20–38.

Lea, D.W., Pak, D.K., Spero, H.J., 2000. Climate impact of Late Quaternary equatorial Pacific sea surface temperature variations. Science 289, 1719–1724.

Martinson, D.G., Pisias, N.G., Hays, J.D., Imbrie, J., 1987. Age dating and the orbital theory of the ice ages: development of a high-resolution 0 to 300,000-year chronostratigraphy. Quat. Res. 27, 1–29.

NGRIP Project members, 2004. High-resolution record of Northern Hemisphere climate extending into the last interglacial period. Nature 431, 147–151.

Porter, S.C., An, Z.S., 1995. Correlation between climate events in the North Atlantic and China during the last glaciation. Nature 375, 305–308.

Shackleton, N.J., 1987. Oxygen isotopes, ice volume and sea level. Quat. Sci. Rev. 6, 183–190.

Shao, X.H., Wang, Y.J., Cheng, H., Kong, X.G., Wu, J.Y., 2006. Long-term trend and abrupt events of the Holocene Asian monsoon inferred from a stalagmite $\delta^{18}O$ record from Shennongjia in Central China. Chin. Sci. Bull. 51 (2), 221–228.

Sinomaps Press, 1984. Atlas of the People's Republic of China. Sinomaps Press, Beijing.

Tan, M., Cai, B.G., 2005. Preliminary calibration of stalagmite oxygen isotopes from eastern monsoon China with Northern Hemisphere temperatures. Pages News 13 (2), 16–17.

Wang, Z., Mysak, L.A., 2006. Glacial abrupt climate changes and Dansgaard–Oeschger oscillations in a coupled climate model. Paleoceanography 21, PA2001. doi:10.1029/2005PA001238.

Wang, Y.J., Cheng, H., Edwards, R.L., An, Z.S., Wu, J.Y., Shen, C.C., Dorale, J.A., 2001. A high-resolution absolute-dated late Pleistocene monsoon record from Hulu Cave, China. Science 294, 2345–2348.

Wang, Y.J., Cheng, H., Edwards, R.L., He, Y.Q., Kong, X.G., An, Z.S., Wu, J.Y., Kelly, M.J., Dykoski, C.A., Li, X.D., 2005. The Holocene Asian monsoon: links to solar changes and North Atlantic climate. Science 308, 854–857.

Wang, Y.J., Cheng, H., Edwards, R.L., Kong, X.G., Shao, X.H., Chen, S.T., Wu, J.Y., Jiang, X.Y., Wang, X.F., An, Z.S., 2008. Millennial- and orbital-scale changes in the East Asian monsoon over the past 224,000 years. Nature 451, 1090–1093.

Wu, W.X., Liu, T.S., 2004. Possible role of the "Holocene Event 3" on the collapse of Neolithic cultures around the central plain of China. Quat. Int. 117, 153–166.

Yuan, D.X., Cheng, H., Edwards, R.L., Dykoski, C.A., Kelly, M.J., Zhang, M.L., Qing, J.M., Lin, Y.S., Wang, Y.J., Wu, J.Y., Dorale, J.A., An, Z.S., Cai, Y.J., 2004. Timing, duration, and transitions of the Last Interglacial Asian monsoon. Science 304, 575–578.

Zhang, X.P., Yao, T.D., 1998. Distributional features of $\delta^{18}O$ in precipitation in China. Acta Geogr. Sin. 53 (4), 356–364 (in Chinese).

Zhao, J.X., Hu, K., Collerson, K.D., Xu, H.K., 2001. Thermal ionization mass spectrometry U-series dating of a hominid site near Nanjing, China. Geology 29, 27–30.

Zhou, H.Y., Li, T.G., Jia, G.D., Zhu, Z.Y., Chi, B.Q., Cao, Q.Y., Sun, R.T., Peng, P.A., 2007. Sea surface temperature reconstruction for the middle Okinawa Trough during the last glacial–interglacial cycle using C37 unsaturated alkenones. Palaeogeogr. Palaeoclimatol. Palaeoecol. 240, 440–453.

Zhou, H.Y., Zhao, J.X., Feng, Y.X., Gagan, M.K., Zhou, G.Q., Yan, J., 2008. Distinct climate change synchronous with Heinrich event one, recorded by stable oxygen and carbon isotopic compositions in stalagmites from China. Quat. Res. 69, 306–315.